ACS OMEGA

Cite This: ACS Omega 2020, 5, 31−40

Mini-Review

http://pubs.acs.org/journal/acsodf

Recent Advances in Noble Metal (Pt, Ru, and Ir)-Based Electrocatalysts for Efficient Hydrogen Evolution Reaction

Changqing Li and Jong-Beom Baek*

School of Energy and Chemical Engineering, Center for Dimension-Controllable Organic Frameworks, Ulsan National Institute of Science and Technology (UNIST), 50 UNIST, Ulsan 44919, South Korea

ABSTRACT: Noble metal (Pt, Ru, and Ir)-based electrocatalysts are currently considered the most active materials for the hydrogen evolution reaction (HER). Although they have been associated with high cost, easy agglomeration, and poor stability during the HER reaction, recent efforts to intentionally tailor noble-metal-based catalysts have led to promising improvements, with lower cost and superior activity, which are critical to achieving large-scale production of pure hydrogen. In this mini-review, we focus on the recent advances in noble-metal-based HER electrocatalysts. In particular, the synthesis strategies to enhance cost-effectiveness and the catalytic activity for HER are highlighted.

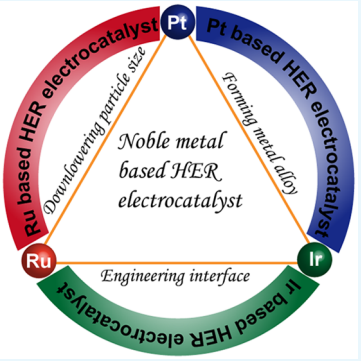

1. INTRODUCTION

The hydrogen evolution reaction (HER) from water electrolysis is considered the most promising approach for acquiring clean and renewable hydrogen energy.[1,2] However, the HER's large overpotential and undesirable kinetics impede its practical application. More efficient catalysts are needed to improve HER performance and achieve higher efficiency.[3−6] Despite that tremendous efforts are paid to find more efficient electrocatalysts for hydrogen production, noble-metal-based materials remain the most efficient HER catalysts.[7] Platinum (Pt), ruthenium (Ru), and iridium (Ir) in particular not only possess high intrinsic electrocatalytic activity but also can be effectively combined with other materials for superior catalytic performance.[1,8] Hence, tailoring these noble-metal-based catalysts is considered crucial to rapidly developing a hydrogen economy in the near future.

Noble-metal-based catalysts have inherent problems, mainly of limited reserve and poor stability.[2,3] Scientists have developed several methods to address these issues, for example, by downsizing the noble metals to single atoms anchored on a porous conductive carbon-based matrix, by forming alloys or by hybridizing with other inexpensive transition metals.[7,9] In addition, interface engineering strategies have also been employed to resolve their high price and instability.[11] These approaches may allow reliable industrial-scale hydrogen production.

In this mini-review, we discuss recent developments in noble metal (Pt, Ru, and Ir)-based catalysts for electrochemical HER, with the primary focus on synthesis strategies and performance-improving factors. Density functional theory (DFT) calculations, which are being used as a powerful tool to reveal the HER mechanisms of catalysts, are highlighted. Last, some of the remaining challenges and promising research directions of these noble-metal-based materials are presented.

2. GENERAL PRINCIPLE OF HYDROGEN EVOLUTION REACTION

The hydrogen evolution reaction (HER) has aroused enormous research interest among chemists and materials scientists because of its potential role in efforts to address the coming energy crisis and critical environmental issues. The HER produces molecular hydrogen from water via different pathways under different pH conditions. In alkaline media, hydrogen intermediates (H_{ad}) are initially formed by the discharge of water in the Volmer step ($H_2O + e^- + \text{catalyst} = \text{catalyst}-H_{ad} + OH^-$), followed by the Heyrovsky step ($H_2O + \text{catalyst-}H_{ad} + e^- = \text{catalyst} + H_2 + OH^-$) or the combined Tafel step ($2\text{catalyst-}H_{ad} = \text{catalyst} + H_2$).[5,12] The reaction pathway is similar in acidic electrolytes, except for the formation of catalyst-H_{ad}, which involves the discharge of hydrogen ions ($H^+ + \text{catalyst} + e^- = \text{catalyst-}H_{ad}$).[9] The HER basically occurs via a Volmer−Heyrowsky pathway or the Volmer−Tafel route. Both reaction pathways involve the adsorption of hydrogen atoms to form hydrogen intermediates (H_{ad}) on the surface of the catalyst. As originally reported by Parsons, the adsorption of H_{ad} subsequently becomes the rate-determining step (RDS) of the entire HER mechanism.[13] However, too weak or too strong hydrogen bond formation can result in a lower reaction rate, by, respectively, affecting the initial hydrogen adsorption process or the ultimate molecular hydrogen desorption from the catalyst surface.[2,12] Accordingly,

Received: October 23, 2019
Accepted: December 5, 2019
Published: December 18, 2019

DOI: 10.1021/acsomega.9b03550
ACS Omega 2020, 5, 31−40

an ideal HER catalyst should possess hydrogen adsorption energies (ΔG_H) approaching $\Delta G_H = 0$.[8,14]

This principle has guided the development of HER catalysts. The volcano plot shown in Figure 1 presents observations from experimental and theoretical calculation studies and illustrates the HER exchange currents and the metal−hydrogen bond strengths of various metals. The volcano plot predicts that the Pt-group metals (Pt, Ru, and Ir) have appropriate surface properties and will be the most promising HER catalysts.[2,12,14]

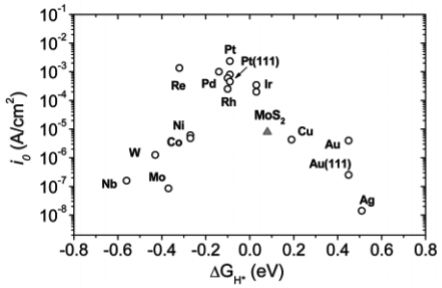

Figure 1. Exchange current density as a function of the hydrogen adsorption energy (ΔG_H) of metal−hydrogen bonds for various pure metals. The experimental "volcano plot" indicates that Pt, with the most approachable zero hydrogen absorption energy, has the highest HER catalytic activity. Reprinted from the work of Chorkendorff et al.[1] Copyright 2007 American Association for the Advancement of Science.

Recently, enormous progress has also been made on non-noble-metal-based electrocatalysts.[3−5] However, noble-metal-based hybrids are thus far still preferred because of their superior activity, and they can be practically adopted to meet industrial hydrogen production demands.[15] The main obstacle to the commercial application of noble metal electrocatalysts is their high cost. Recently, cost issues have been greatly alleviated by reducing mass loading or by forming alloys with other inexpensive metals.[16,17] Other measures, including downsizing the particle size and engineering active crystalline facets at the interface to enhance utilization efficiency, have also been explored.[18,19] Both strategies have demonstrated the unexpected effect of improving activity while lowering the integrated cost of the noble metal electrocatalysts. We will discuss these points in more detail in the following section.

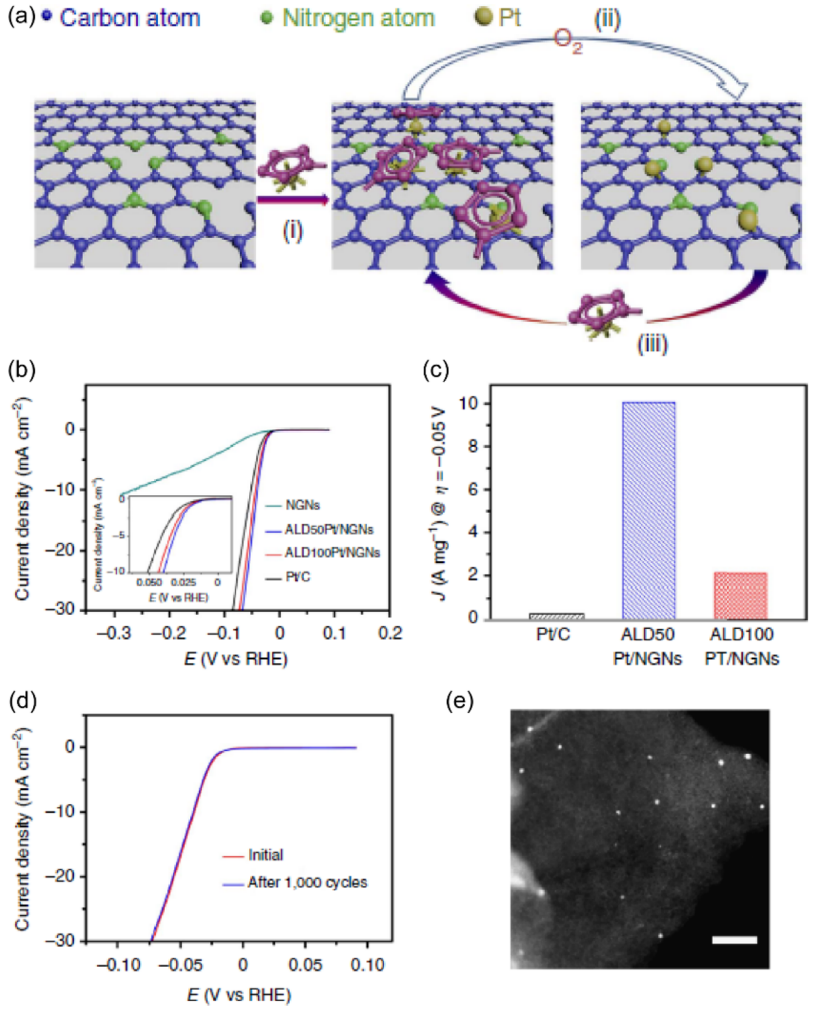

Figure 2. (a) Schematic of the formation of single Pt atoms on NDNs using the ALD cycle process. (b) HER catalytic activity evaluation for ALD Pt/NGNs and Pt/C benchmark catalysts in 0.5 M H_2SO_4. (c) Mass activity comparison of Pt/C and ALD Pt/NGNs obtained from 50 and 100 ALD cycles. (d) Stability response of ALD50Pt/NGNs before and after 1000 cyclic voltammetry cycles. (e) ADF STEM images of ALD50Pt/NGNs captured after the complete ALD process. Reproduced with permission from ref 18. Copyright 2015 Nature Publishing Group.

DOI: 10.1021/acsomega.9b03550
ACS Omega 2020, 5, 31−40

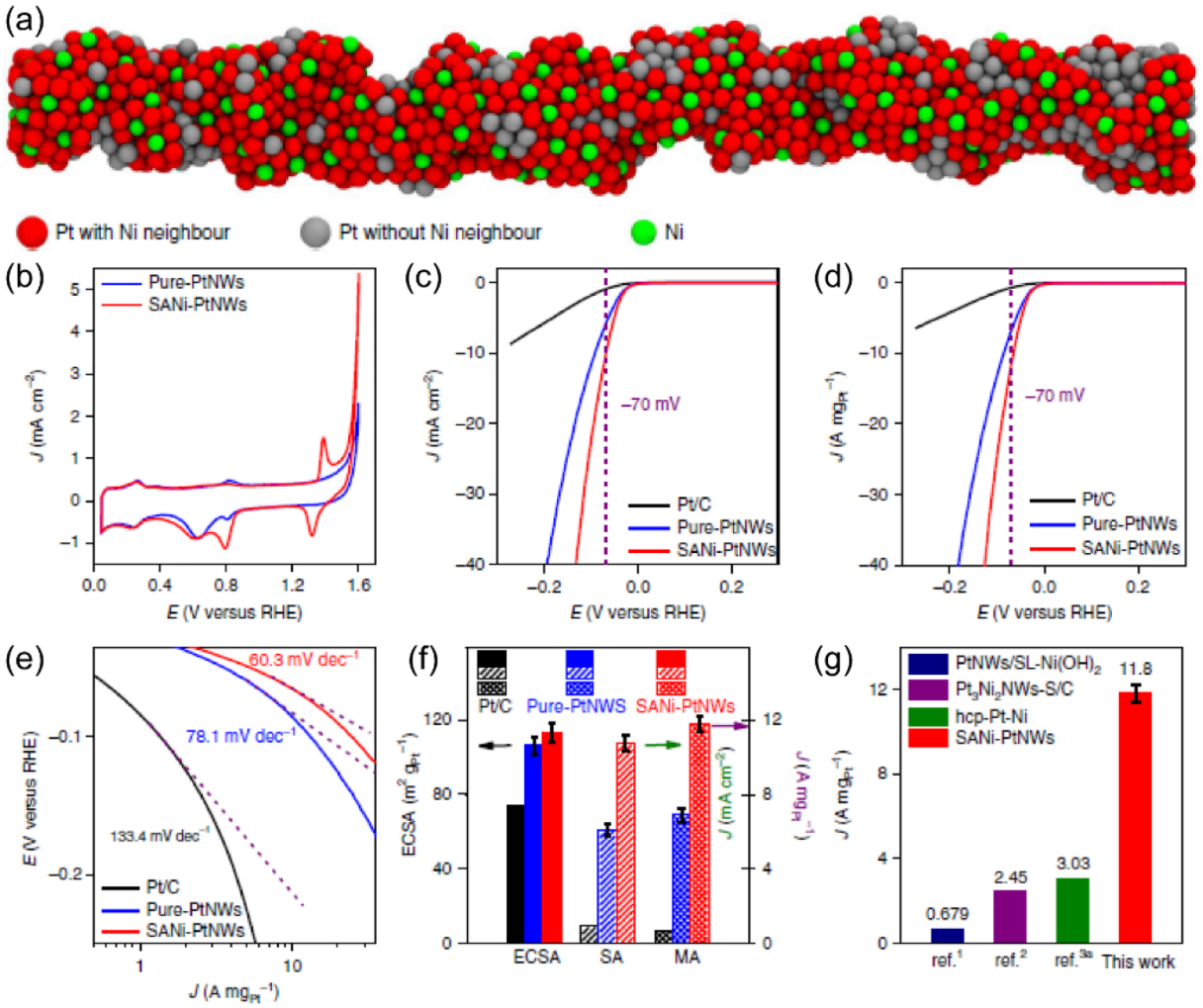

Figure 3. (a) Structural diagram of single atomic nickel species on ultrafine Pt nanowires (SANi-PtNWs). (b) Cyclic voltammetry curves of SANi-PtNWs and pure-PtNWs. LSV curves obtained by normalizing (c) ESCA and (d) Pt mass loading, (e) Tafel slope plot normalized by Pt mass loading, and (f) ECSA and special activity comparison of SANi-PtNWs, pure-PtNWs, and commercial Pt/C. (g) Mass activity comparison of SANi-PtNWs with those reported catalysts. Reproduced with permission from ref 7. Copyright 2019 Nature Publishing Group.

3. NOBLE-METAL-BASED HER CATALYSTS

3.1. Platinum (Pt)-Metal-Based Catalysts. Platinum (Pt) exhibits the highest HER activity and is widely preferred as an active HER catalyst for H_2 production.[11,16] The main obstacle to its industrial application is its high cost and poor stability in corrosive electrolytes. The most promising strategy has therefore been to find ways to reduce the loading amount of Pt while retaining its high efficiency.[7,8] Recently, Pt nanoparticles supported on carbon-based composites are developed as a promising way to enhance their catalytic activity toward HER.[15] The carbon materials can be precisely controlled to obtain a desirable nanostructure with high specific surface area. This serves as the ideal matrix to support the Pt nanoparticles (NPs), providing abundant active sites.[3,12,16] Moreover, when using Pt-supported carbon-based hybrids, the substrate's enhanced electrical conductivity allows fast electron transfer for HER kinetics. Superior catalytic activity can be induced by the strong interaction with, and synergistic effect of, the metallic species and the carbon supports, which also effectively prevents agglomeration and leaching of the Pt NPs during the electrochemical process.[16]

Citing the advantageous synergistic effects of the carbon matrix, Sun et al.[18] prepared single Pt atoms and clusters on a nitrogen-doped graphene nanosheet (NGN) matrix (ALD Pt/NGN) as a HER catalyst, using the controllable atomic layer deposition (ALD) method. A Pt precursor was initially anchored on the NGN substrates, and then a Pt-containing monolayer was formed under the oxidative environment (Figure 2a). After the continuous anchoring and oxidizing processes, the size distribution of Pt catalysts can be precisely controlled by the self-limiting surface reactions of the ALD. Figure 2b compares the HER activity of NGN, commercial Pt/C, and ALDPt/NGN prepared under 50 and 100 ALD cycles. The ALD50Pt/NGN and ALD100Pt/NGN exhibited superior HER activity over Pt/C, and a lower Tafel slope value of 29 mV dec^{-1} was achieved with the ALDPt/NGN catalysts. Mass activity (MA) was normalized with Pt loading and confirmed the ALD50Pt/NGN sample had the highest HER performance, considering an available 10.1 A mg^{-1} MA parameter with a Pt loading as low as 2.1 wt %. The MA value of ALD50Pt/NGN also outperformed ALD100Pt/NGN (2.12A mg^{-1}) and a Pt/C catalyst (0.27A mg^{-1}).

Such results suggest that the single Pt atom and clusters can remarkably enhance Pt utilization efficiency compared with other NPs and reduce the integrated cost of HER catalysts.

DOI: 10.1021/acsomega.9b03550
ACS Omega 2020, 5, 31−40

Stability, which is one of the crucial factors in catalyst evaluation, was also probed. The ALD50Pt/NGN exhibited almost the same LSV curve before and after 1000 cyclic voltammetry cycles. Scanning transmission electron microscopy (STEM) images of the ALDPt/NGN after accelerated degradation tests indicated the Pt particle size had slightly increased, but no aggregation was observed, further confirming the robust stability of ALDPt/NGN for HER.

The metal alloying process has emerged as another promising technique for advancing Pt-based HER catalysts. A Pt-based bimetallic system formed by decoration of other transition metal species on Pt-based materials has also been reported.[9] Bimetallic alloy catalysts have been shown to acquire unprecedented electronic and chemical properties, which are distinctively different from their parent metals.[20] Fundamental surface science research conducted on bimetallic catalysts has proven that the modification is crucial to the unexpected property, which originates from a change in heteroatom bonds and the novel nanostructure within the bimetallic system. These factors endow Pt-based metallic catalysts with excellent activity.[15,20]

Duan et al.[7] synthesized single-atom nickel-modified Pt nanowires (SANi-PtNWs) by partially dealloying PtNi alloy nanowires. The formed SANi-PtNWs had abundant activated Pt sites adjacent to single-atom Ni and minimal blocked Pt sites on the surface, which led to the highest mass activity (MA) (Figure 3a). The cyclic voltammetry tests of SANi-PtNWs suggested the appearance of two new redox peaks (Ni^{2+}/Ni^{3+}) at around 1.32 and 1.34 V, compared with pure-PtNWs. This suggests the successful decoration of nickel species on PtNWs (Figure 3b). A linear sweep voltammetry (LSV) evaluation conducted in 1 M N_2-saturated KOH electrolyte revealed that the SANi-PtNWs possessed the highest specific activity (SA), MA, and the lowest Tafel slope value (Figure 3c–f), of 10.72 ± 0.41 mA cm^{-2}, 11.80 ± 0.43 A mg_{Pt}^{-1}, and 60.3 mV dec^{-1}, respectively, over pure-PtNWs (6.11 ± 0.34 mA cm^{-2}, 6.90 ± 0.36 A mg_{Pt}^{-1}, 78.1 mV dec^{-1}) and Pt/C (0.95 mA cm^{-2}, 0.71 A mg_{Pt}^{-1}, 133.4 mV dec^{-1}) catalysts. This clearly demonstrates the remarkably enhanced HER kinetics of the single-atom decorated alloy.

With the highest ECSA and SA values, the SANi-PtNWs achieved a leap in MA value, of ∼3−10 times higher MA, surpassing many superior HER catalysts (Figure 3g).

DFT calculations indicated that the single nickel atoms electronically modified the neighboring Pt atoms, lowering their metal−hydrogen bonding energy barrier to the range of the best HER activity.

The engineering of active crystalline facets is another promising technique being used to rationally design efficient Pt-based HER catalysts. In an early report, Markovic et al.[21] indicated that Pt surfaces exhibited facet-oriented HER activity in alkaline media. They suggested that this activity mainly resulted from the structure-sensitive blockage of overpotential deposition on H (H_{opd}) and the adsorption of HO^- (OH_{ad}) species on different Pt facets. The activity of the Pt facets followed the order of Pt(110) > Pt(100) > Pt(111).[8,21]

However, constructing monocrystalline noble metals with a well-defined surface structure is not always feasible, even with a commonly used sacrificial templated method.[15] In that case, introducing other active species to tune the active Pt-rich facets may result in superior activity. Huang et al.[15] developed platinum−nickel/nickel sulfide heterostructures (Pt_3Ni_2 NWs-S/C) with a composition-segregated feature. The active Pt(111) facets were greatly promoted after incorporating Ni, forming $Pt_3Ni(111)$ facets. Interfacial NiS species can trigger positive synergistic effects on Pt_3Ni with various activity. DFT calculations suggest that the hydrogen binding energy G_{H^*} of $Pt_3Ni(111)$ is almost identical to the value for Pt(111). Once the $Pt_3Ni(111)$ combines with the NiS(100) crystalline facet, the water dissociation step and H_{ads} adsorption can be balanced, to achieve exceptional HER activity in alkaline environments (Figure 4).

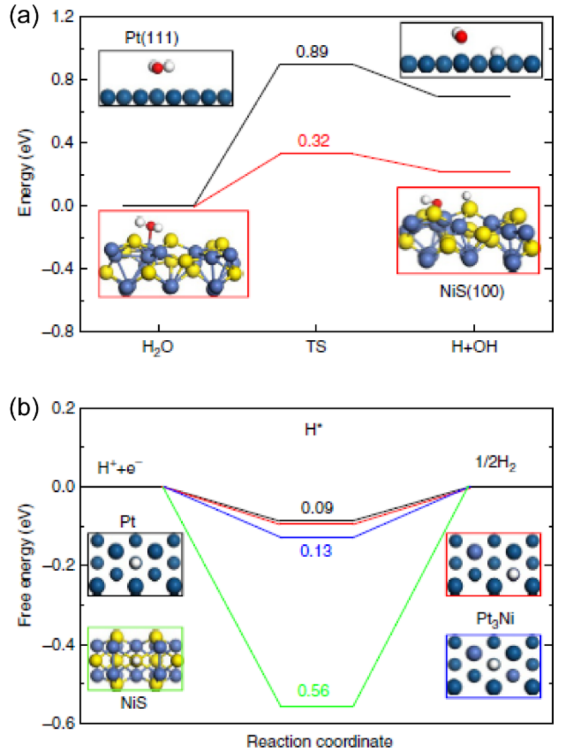

Figure 4. (a) DFT calculations of the water cleavage energy diagram on Pt(111) and NiS(100) facets. (b) Reaction free energy diagram of HER on Pt(111), NiS(100), and Pt_3Ni (111) facets. Reproduced with permission from ref 15. Copyright 2017 Nature Publishing Group.

3.2. Ruthenium (Ru)-Metal-Based Catalysts. As an inexpensive and viable alternative to Pt, ruthenium (Ru) has similar metal-hydrogen-bond strength (∼65 kcal mol^{-1}),[22] and this enables Ru to exhibit HER activity that is comparable to or even superior to Pt. Rare studies have reported a pH-universal application of Ru toward HER. Beak et al.[22] prepared Ru on a nitrogenated holey two-dimensional C_2N structure (Ru@C_2N) catalyst. The C_2N framework serves as a versatile platform for the adsorption, nucleation, and growth of Ru nanoparticles (NPs), and it also provides abundant coordination sites for the distribution of small size Ru NPs within the C_2N layers (Figure 5a). The as-prepared Ru@C_2N catalyst was first tested in a 0.5 M H_2SO_4 solution to evaluate HER performance. The Ru@C_2N required the low overpotential of 22 mV to deliver a current density of 10 mA cm^{-2}, which is close to that of Pt/C (16 mV) and superior to Co@C_2N (290 mV), Ni@C_2N (410 mV), Pd@C_2N (330 mV), and Pt@C_2N (60 mV) samples (Figure 5b,c). The small Tafel slope value suggests that Ru@C_2N follows a Volmer−Tafel reaction mechanism.

Changing the tested solution from acid to alkaline, the Ru@C_2N exhibited even higher activity with an accessible low overpotential of 17 mV, to reach the benchmark 10 mA cm^{-2}

DOI: 10.1021/acsomega.9b03550
ACS Omega 2020, 5, 31−40

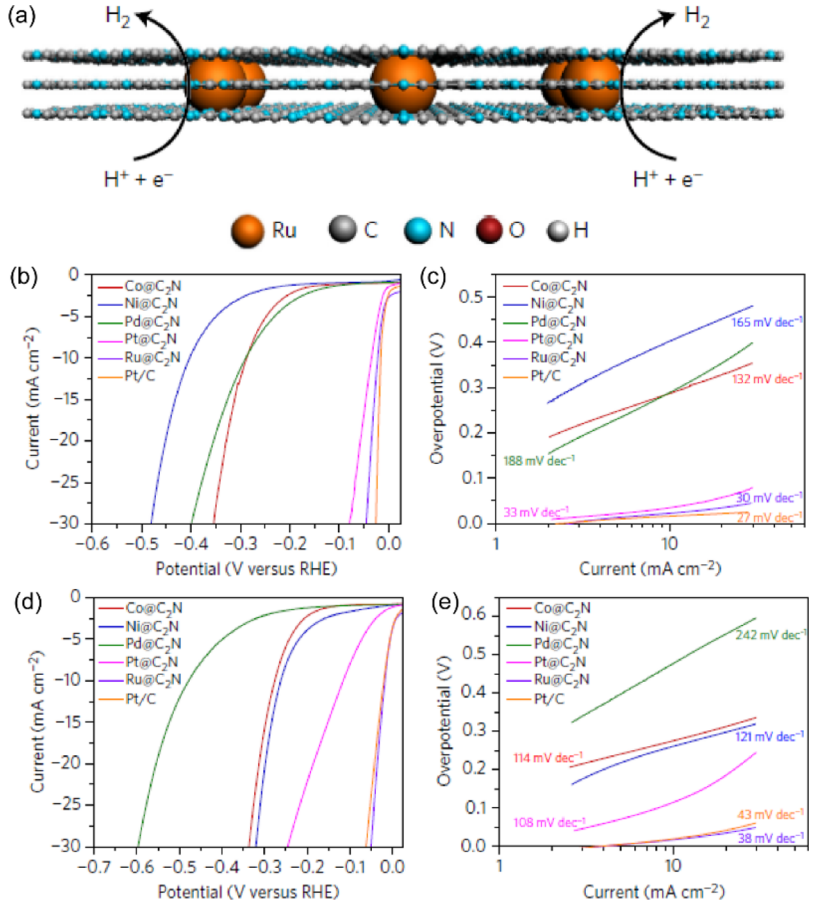

Figure 5. (a) Molecular structure of Ru@C_2N, formed by supporting nanosized Ru on a C_2N framework. LSV curves and Tafel plots of Co@C_2N, Ni@C_2N, Pd@C_2N, Pt@C_2N, and commercial Pt/C in (b,c) 0.5 M H_2SO_4 solution and (d,e) 1.0 M KOH solution. Panels a–e reproduced with permission from ref 22. Copyright 2017 Nature Publishing Group.

and small Tafel slope of 38 mV dec^{-1}, compared with Pt/C (20.7 mV, 43 mV dec^{-1}) (Figure 5d,e).

DFT calculations provide more information about the differences in the activity of the Ru@C_2N in different pH environments. In an acid solution, the Ru@C_2N possesses a hydrogen binding energy (0.55 eV H^{-1}) that is very similar to that of the active Pt(111) surface, whose value is typically regarded as the optimal binding energy to efficiently facilitate proton adsorption, reduction, and gas desorption. On the other hand, in alkaline media, the Ru@C_2N reaction proceeds by a different mechanism. The Ru@C_2N surface has fast H_2O adsorption ability and cleaves the adsorbed H_2O into H and OH and then rapidly transports the proton required for the following reaction step. This favorably compensates the loss in efficiency during the Volmer step produced by the strong OH binding.

In their latest work, Huang et al.[23] incorporated Ru with a transition metal copper (Cu) to form channel-rich RuCu snowflake-like nanosheets (NSs) (Figure 6a). The accessible channels within the 2D nanosheets (Figure 6b) contributed to its improved electrocatalytic performance, which resulted from increased surface area, boosted mass, and electron transfer ability.

DFT calculations confirmed the surface electronic activation of the channel-rich area, and the critical importance of the synergistic effect was exerted by amorphous Cu on crystallized Ru species, which were responsible for the superior catalytic activity. In the adjacent channel area, short-range disorder lowers the intermediate energetic cost produced by the bond dissociation of lattice relaxation.

The PDOS plot demonstrated that the coexistence of a broad range of electron-rich features within the Ru 4d bands and the electron-rich states of the Cu 3d bands in RuCu NSs was beneficial to the rapid electron transfer between the Ru and adsorbates.

To optimize HER performance, the RuCu NSs were loaded on carbon black and annealed at different temperatures. The as-synthesized RuCu NSs/C-250 °C exhibited the best HER activity in both acid and alkaline electrolytes. The RuCu NSs/C-250 °C required low overpotentials of 20, 40, 19, and 27 mV to reach 10 mA cm^{-2} in 1.0 M KOH, 0.1 M KOH, 0.5 M H_2SO_4, and 0.05 M H_2SO_4 test solutions.

Other samples including RuCu NPs/C-250 °C, Ir/C, and Pt/C were inferior to the RuCu NSs/C-250 °C. Specifically, RuCu NSs/C-250 °C possessed small Tafel slopes of 15.3 and 22.3 mV dec^{-1} in 1 M KOH and 0.1 M KOH solutions, much lower than Pt/C (39.8 and 42.0 mV dec^{-1}), proving the dominant HER kinetics of RuCu NSs/C-250 °C in the alkaline pathway.

In addition to directly participating in the HER reaction, Ru has also been proposed in efforts to produce beneficial modulation effects to enhance HER activity. Dai and co-workers[11] developed pod-like Ni@Ni_2P–Ru catalysts for HER catalysis in a wide range of pH conditions. They first employed DFT calculations to predict the positive effect of incorporating Ru into Ni_2P species. The simulated Ni_2P–Ru cluster (Figure

DOI: 10.1021/acsomega.9b03550
ACS Omega 2020, 5, 31−40

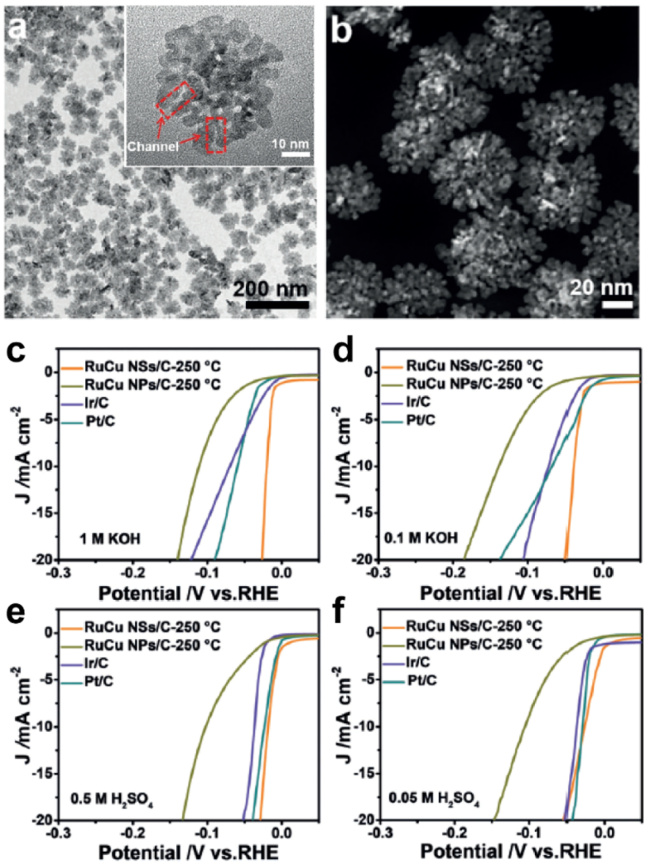

Figure 6. (a) TEM image and (b) HAADF-STEM image (inset: HRTEM images) of RuCu NSs. Polarization curves of RuCu/C-250 °C with different morphologies, Ir/C and Pt/C in (c) 1.0 M KOH, (d) 0.1 M KOH, (e) 0.5 M H_2SO_4, and (f) 0.05 M H_2SO_4. Panels a–f reprinted with permission from ref 23. Copyright 2019 John Wiley & Sons, Inc.

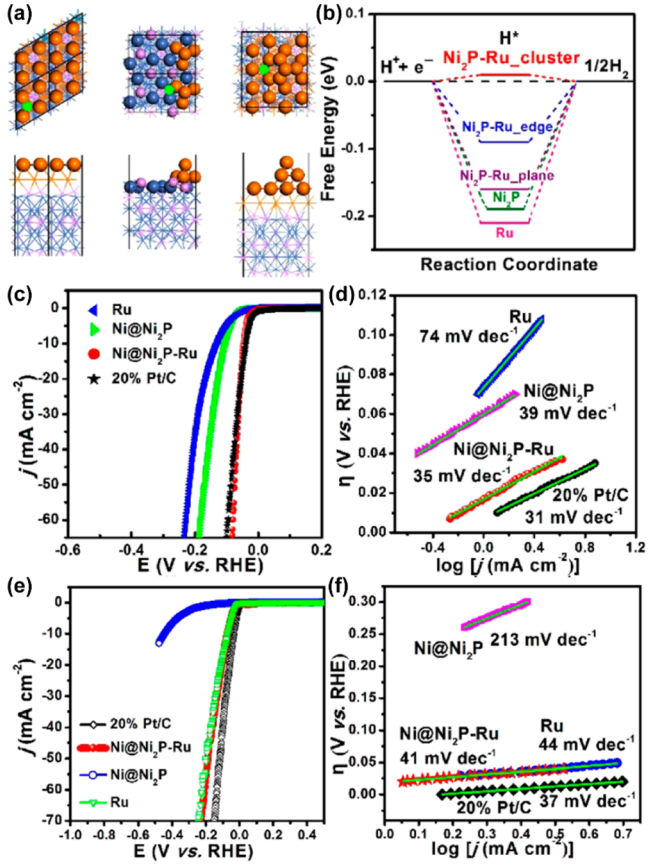

Figure 7. (a) Proposed structure of Ni_2P–Ru viewed from different directions, the plane, edge, and Ni_2P–Ru cluster. (b) The calculated reaction free energy diagrams of optimized Ni_2P–Ru, Ni_2P, and Ru, respectively. HER polarization curves and Tafel plot curves of Ni@Ni_2P–Ru, Ni@Ni_2P, Pt/C, and Ru in (c,d) 0.5 M H_2SO_4 and (e,f) 1.0 M KOH. Reproduced with permission from ref 11. Copyright 2018 American Chemical Society.

7a) almost reached the optimal adsorption free energy of intermediate H* with the ΔG_{H^*} value of 0.01 eV (Figure 7b).

Encouraged by the theoretical prediction, a multiheterogeneous Ni@Ni_2P–Ru nanorod was then prepared. Synchrotron-based X-ray absorption fine structure (XANES and EXAFS) measurements suggested that the introduction of Ru into Ni@Ni_2P can modulate the phosphatization process of Ni, through a Ru–Ni coordination effect.

Meanwhile, the introduced Ru is extremely beneficial to the retention of metallic Ni, which ensures great conductivity in a satisfactory catalyst system. The evaluation of electrocatalytic activity confirmed that the Ni@Ni_2P–Ru possessed excellent HER activity in both acid and alkaline electrolytes. The Ni@Ni_2P–Ru required low overpotentials of 51 and 41 mV, respectively, to obtain 10 mA cm^{-2}, and showed small Tafel slopes of 35 mV dec^{-1} and 41 mV dec^{-1} in 0.5 M H_2SO_4 and 1.0 M KOH.

3.3. Iridium (Ir)-Metal-Based Catalysts. Iridium (Ir), with its weak hydrogen binding energy, was first selected for the chemisorption of hydrogen.[24] In a hydrogen adsorption/desorption test, Ir with a specific (111) facet is thermally stable and exhibits relatively balanced hydrogen adsorption/desorption capacity, comparable to Pt(100).[24] Its position near the top of the HER volcano plot ensures that Ir receives considerable attention as a viable alternative to Pt.[2,14]

Both experiments and theoretical calculations have confirmed that having optimal hydrogen adsorption energy is a prerequisite for an efficient HER catalyst, depending on the HER reaction mechanism.[14] Probing the hydrogen adsorption/desorption behaviors of catalysts is thus crucial for the development of active HER catalysts.[12,23] Li et al.[25] chose Ir(111) as a theoretical model to study its behavior of hydrogen chemisorption. Ir NPs can be tailored using an electronegative carbon/nitrogen (C/N) matrix, exposing an Ir(111) crystalline facet. A previous study suggested that d orbitals have a huge effect on hydrogen adsorption/desorption on the surface of transition metals.[20] The projected DOS distributions with hydrogen adsorbates, Ir and IrNC, reveal that the surficial Ir sites on IrNC have stronger hydrogen bonding (Figure 8a–c).

Considering the whole HER reaction pathway, the large upslope value of 0.25 eV at Ir sites can be reduced to 0.04 eV by balancing the electronegative environment with C/N sites. This is even lower than the value for Pt (0.09 eV). In that case, the hydrogen bonding energy on the surface of IrNC would be better optimized to be more favorable for the hydrogen adsorption/desorption in water splitting.

To date, considerable progress has been achieved using DFT calculations and ultrahigh vacuum (UHV) experiments on bimetallic surfaces.[10,20] One of the notable discoveries is that a

DOI: 10.1021/acsomega.9b03550
ACS Omega 2020, 5, 31–40

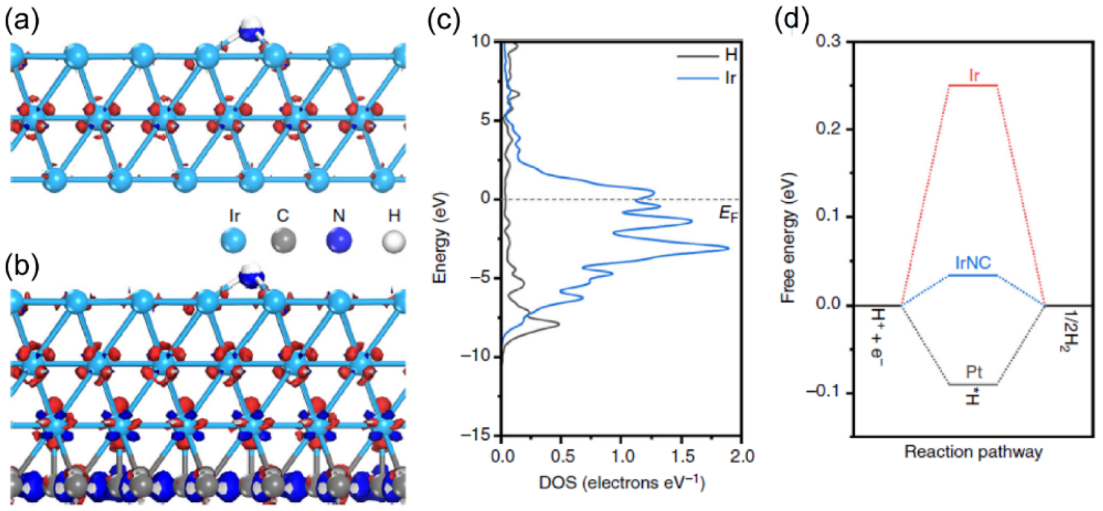

Figure 8. Theoretical calculations for hydrogen adsorption on Ir and IrNC. (a,b) The variation in electron density on the surface of Ir and IrNC in relation to H adsorption. (c) Density of states (DOS) of the surface-adsorbed H on the Ir sites of IrNC. (d) Free energy diagram of Ir and IrNC. Reproduced with permission from ref 25. Copyright 2019 Nature Publishing Group.

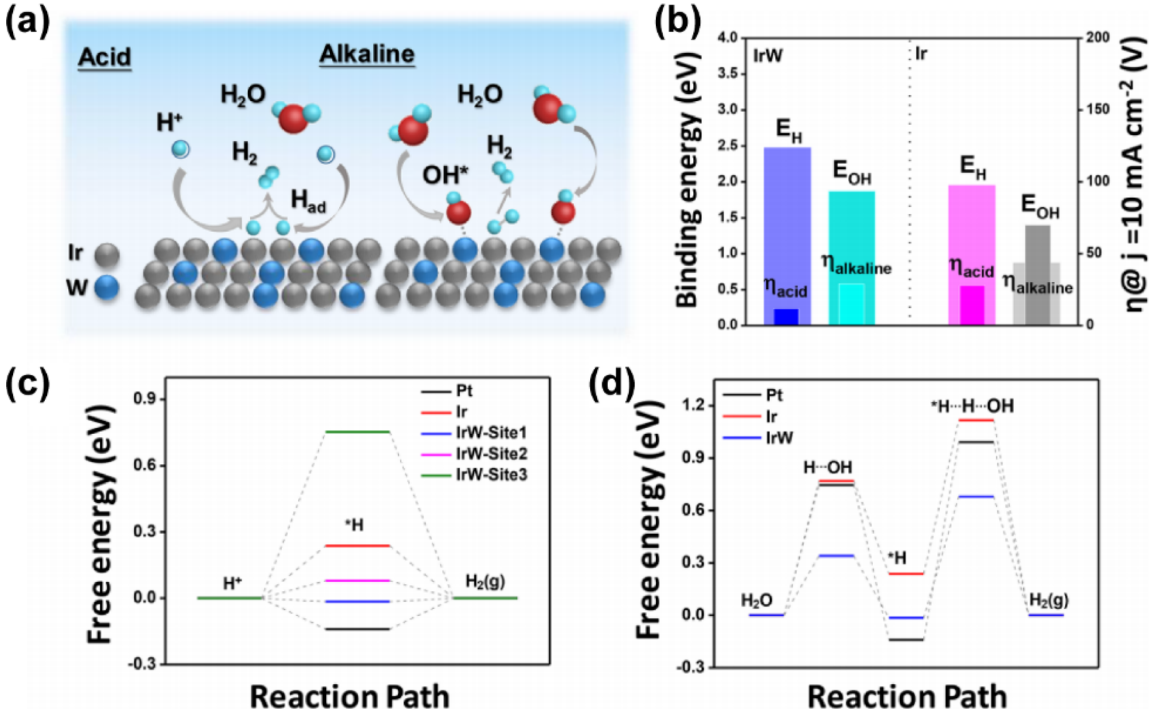

Figure 9. Reaction mechanism of IrW NDs toward HER in acidic and alkaline solutions. (a) Schematic HER reaction step on the surface of IrW NDs in acidic and alkaline environments. (b) Trends in HER performance under varied H and OH binding energies. (c) HER free energy diagram of Pt, Ir, and IrW at different reaction sites. (d) Free energy diagram of the alkaline Volmer−Heyrosky pathway. Reproduced with permission from ref 17. Copyright 2018 American Chemical Society.

monolayer admetal will interact with a parent metal substrate, modifying the surface d-band center, which further influences the adsorption energy of bimetallic structures, enabling access to unprecedented chemical properties. Guo et al.[17] reported an Ir-tungsten (W) alloy with a nanodendritic structure (IrW ND) as an efficient catalyst toward a pH-universal HER application. Because of the different HER mechanisms in acid and alkaline conditions (Figure 9a), free energy diagrams based on first-principles calculations were separately developed to investigate the superior HER activity on IrW NDs. Using the binding energies of H (E_H) and OH (E_{OH}) as an indicator (Figure 9b), the IrW-Site1 was determined to have a weaker binding energy than Pt (Figure 9c). Its moderate strength makes IrW a promising catalyst in acid environments, according to the Sabatier principle.[26]

Likewise, the IrW also exhibited lower binding energies of 0.34 and 0.61 eV, respectively, for water dissociation and dissociated OH bonding energy (Figure 9d), outperforming Pt (0.75 and 0.88 eV) and Ir (0.77 and 1.13 eV). The lower barrier value of IrW is associated with the stronger affinity of the W active site to OH in alkaline conditions. In combination, these features enabled IrW to exhibit better HER activity than Pt or Ir in both acidic and alkaline environments. This result was also supported by DFT calculations, which confirmed the

DOI: 10.1021/acsomega.9b03550
ACS Omega 2020, 5, 31−40

stronger adsorption of H on Ir active sites and the higher affinity of OH to the surface W of IrW.

Except for the metal−metal interaction, which is responsible for enhanced HER catalytic activity, the heteroatom is also suggested as a crucial component to tune the electrocatalytic performance of the noble-metal-based electrocatalyst because of its intrinsic electronegativity. Nitrogen-doped porous carbon not only serves as an ideal matrix to anchor and prevent aggregation of active noble metal atoms/particles during the pyrolysis process but also coordinates with the noble metal atom to modify the electronic structure of the catalyst. Nanosized iridium nanoparticles loaded on nitrogen-doped graphene sheets (Ir@N-G-750) are reported with pronounced HER activity in both acidic and alkaline conditions.[27] Unlike the well-acknowledged role emphasized on the whole nitrogen atom, a specific type of N atom is reported to effectively affect the interfacial property of Ir.

DFT calculations illustrate that the formation of pyridinic N could remarkably reduce the adhesion energy of nitrogen-doped carbon species (Figure 10a). Once the Ir cluster is

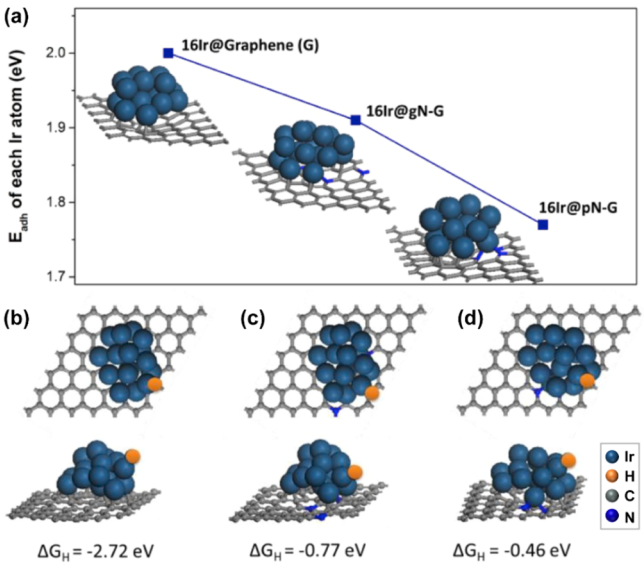

Figure 10. (a) Calculated adhesion energies of pristine graphene, graphitic N-doped graphene, and pyridinic N-doped graphene. Hydrogen-adsorbed energy and different views of Ir cluster anchored (b) pristine graphene, (c) graphitic N-doped graphene, and (d) pyridinic N-doped graphene. Reproduced from ref 27 with permission from Elsevier Inc., Copyright 2019.

introduced into the N−graphene system, the distance of the adjacent N atom is minimized and starts to form the Ir−N site. The Gibbs free energy of hydrogen adsorption on Ir−N is herein tuned by the favorable active pyridinic N (−0.46 eV) adhered on the Ir surface (Figure 10b), compared to the Ir−pyrrole N (−0.77 eV) and the pure Ir−graphene site (−2.72 eV) (Figure 10c,d). Thus, N-doping is beneficial for improved HER electrocatalytic performance.

4. CONCLUSION AND PERSPECTIVES

In this mini-review, we have focused on the most recent developments of noble metal (Pt, Ru, and Ir)-based materials as promising catalysts toward HER. Pt with moderate price and relatively poor stability has been the most widely studied as HER electrocatalysts with superior activity in a wide pH range. Ru with the lowest price and high stability is explored as an excellent HER electrocatalyst to produce hydrogen in both acid and alkaline conditions, specifically when it is on the N-doped porous carbon matrix. Ir with the highest price and stability can be adopted as an ideal model to study the chemisorption of hydrogen during the HER process. Several strategies have been exploited to address the high cost and instability issues of those materials, including downsizing the noble metals to single-atom catalysts, forming alloys, or hybridizing with other inexpensive transition metals and interface engineering. By modifying the catalysts' surface hydrogen adsorption behavior, those methods have greatly improved the performance of noble-metal-based catalysts. Still, challenges remain in the development of highly active noble-metal-based catalysts. For single-atom catalysts (SACs), active sites remain elusive and may originate from the synergistic effect of complex structures on the carbon matrix and the electronic properties of the SACs. In addition, the relatively lower density, easily transferred nature, as well as the undesirable tendency to the aggregation need to be further resolved in SACs. The preparation of noble-metal-based alloys is much more complex and challenging, and many of the proposed bimetallic structures tend to change during the reaction. Thus, identifying the atomic arrangement of alloy catalysts is critical, using some powerful characterization methods, such as in situ spectroscopic or microscopic techniques and/or EXAFS. Interface engineering strategies can lead to metal segregation and diffusion under reaction conditions, especially during long-term stability tests. Further experimental and theoretical efforts are necessary to minimize the gap between water splitting and hydrocarbon reforming, for highly efficient hydrogen production.

AUTHOR INFORMATION

Corresponding Author

*Phone: +82-52-217-2510. Fax: +82-52-217-2019. E-mail: jbbaek@unist.ac.kr.

ORCID

Jong-Beom Baek: 0000-0003-4785-2326

Notes

The authors declare no competing financial interest.

Biographies

Changqing Li is a Ph.D. candidate in the School of Energy and Chemical Engineering, Center for Dimension-Controllable Organic Frameworks, at Ulsan National Institute of Science and Technology (UNIST), South Korea. He received his M.S. degree at Capital Normal University in 2019. His interest focuses on the design of

DOI: 10.1021/acsomega.9b03550
ACS Omega 2020, 5, 31−40

metal-based materials and carbon-based materials for electrochemical applications.

Jong-Beom Baek is a professor and director at the School of Energy and Chemical Engineering, Center for Dimension Controllable Organic Frameworks, at Ulsan National Institute of Science and Technology (UNIST), South Korea. After receiving his Ph.D. from the University of Akron, USA (Polymer Science, 1998), he joined the Wright-Patterson Air Force Research Laboratory (AFRL). He returned to South Korea to take a position as an assistant professor at Chungbuk National University in 2003, before moving to UNIST in 2008. His current research interests include the synthesis of two-dimensional high-performance polymers and chemical modification of carbon-based materials for multifunctional applications.

■ ACKNOWLEDGMENTS

This research was supported by the Creative Research Initiative (CRI, 2014R1A3A2069102), BK21 PLUS (10Z20130011057), and Science Research Center (SRC, 2016R1A5A1009405) programs through the National Research Foundation (NRF) of Korea.

■ REFERENCES

(1) Jaramillo, T. F.; Jørgensen, K. P.; Bonde, J.; Nielsen, J. H.; Horch, S.; Chorkendorff, I. Identification of active edge sites for electrochemical H_2 evolution from MoS_2 nanocatalysts. *Science* **2007**, *317*, 100−102.

(2) Digraskar, R. V.; Sapner, V. S.; Mali, S. M.; Narwade, S. S.; Ghule, A. V.; Sathe, B. R. CZTS decorated on graphene oxide as an efficient electrocatalyst for high-performance hydrogen evolution reaction. *ACS Omega* **2019**, *4*, 7650−7657.

(3) Paul, R.; Zhu, L.; Chen, H.; Qu, J.; Dai, L. Recent advances in carbon-based metal-free electrocatalysts. *Adv. Mater.* **2019**, *31*, 1806403−1806427.

(4) Kumar, R.; Ahmed, Z.; Rai, R.; Gaur, A.; Kumari, S.; Maruyama, T.; Bagchi, V. Uniformly decorated molybdenum carbide/nitride nanostructures on biomass templates for hydrogen evolution reaction applications. *ACS Omega* **2019**, *4*, 14155−14161.

(5) Li, F.; Han, G.; Noh, H.-J.; Ahmad, I.; Jeon, I.-Y.; Baek, J.-B. Mechanochemically assisted synthesis of a Ru catalyst for hydrogen evolution with performance superior to Pt in both acidic and alkaline media. *Adv. Mater.* **2018**, *30*, 1803676−1803683.

(6) Sheng, M.; Jiang, B.; Wu, B.; Liao, F.; Fan, X.; Lin, H.; Li, Y.; Lifshitz, Y.; Lee, S.-T.; Shao, M. Approaching the volcano top: iridium/silicon nanocomposites as efficient electrocatalysts for the hydrogen evolution reaction. *ACS Nano* **2019**, *13*, 2786−2794.

(7) Li, M.; Duanmu, K.; Wan, C.; Cheng, T.; Zhang, L.; Dai, S.; Chen, W.; Zhao, Z.; Li, P.; Fei, H.; Zhu, Y.; Yu, R.; Luo, J.; Zang, K.; Lin, Z.; Ding, M.; Huang, J.; Sun, H.; Guo, J.; Pan, X.; Goddard, W. A., III; Sautet, P.; Huang, Y.; Duan, X. Single-atom tailoring of platinum nanocatalysts for high-performance multifunctional electrocatalysis. *Nat. Catal.* **2019**, *2*, 495−503.

(8) Ruqia, B.; Choi, S.-I. Pt and Pt-Ni$(OH)_2$ electrodes for the hydrogen evolution reaction in alkaline electrolytes and their nanoscaled electrocatalysts. *ChemSusChem* **2018**, *11*, 2643−2653.

(9) Porter, N. S.; Wu, H.; Quan, Z.; Fang, J. Shape-control and electrocatalytic activity-enhancement of Pt-based bimetallic nanocrystals. *Acc. Chem. Res.* **2013**, *46*, 1867−1877.

(10) Saleem, F.; Zhang, Z.; Cui, X.; Gong, Y.; Chen, B.; Lai, Z.; Yun, Q.; Gu, L.; Zhang, H. Elemental segregation in multimetallic core-shell nanoplates. *J. Am. Chem. Soc.* **2019**, *141*, 14496−14500.

(11) Liu, Y.; Liu, S.; Wang, Y.; Zhang, Q.; Gu, L.; Zhao, S.; Xu, D.; Li, Y.; Bao, J.; Dai, Z. Ru modulation effects in the synthesis of unique rod-like Ni@Ni_2P-Ru heterostructures and their remarkable electrocatalytic hydrogen evolution performance. *J. Am. Chem. Soc.* **2018**, *140*, 2731−2734.

(12) Zhou, W.; Jia, J.; Lu, J.; Yang, L.; Hou, D.; Li, G.; Chen, S. Recent developments of carbon-based electrocatalysts for hydrogen evolution reaction. *Nano Energy* **2016**, *28*, 29−43.

(13) Parsons, R. The rate of electrolytic hydrogen evolution and the heat of adsorption of hydrogen. *Trans. Faraday Soc.* **1958**, *54*, 1053−1063.

(14) Benck, J. D.; Hellstern, T. R.; Kibsgaard, J.; Chakthranont, P.; Jaramillo, T. F. Catalyzing the hydrogen evolution reaction (HER) with molybdenum sulfide nanomaterials. *ACS Catal.* **2014**, *4*, 3957−3971.

(15) Wang, P.; Zhang, X.; Zhang, J.; Wan, S.; Guo, S.; Lu, G.; Yao, J.; Huang, X. Precise tuning in platinum-nickel/nickel sulfide interface nanowires for synergistic hydrogen evolution catalysis. *Nat. Commun.* **2017**, DOI: 10.1038/ncomms14580.

(16) Tiwari, J. N.; Sultan, S.; Myung, C. W.; Yoon, T.; Li, N.; Ha, M.; Harzandi, A. M.; Park, H. J.; Kim, D. Y.; Chandrasekaran, S. S.; Lee, W. G.; Vij, V.; Kang, H.; Shin, T. J.; Shin, H. S.; Lee, G.; Lee, Z.; Kim, K. S. Multicomponent electrocatalyst with ultralow Pt loading and high hydrogen evolution activity. *Nat. Energy* **2018**, *3*, 773−782.

(17) Lv, F.; Feng, J.; Wang, K.; Dou, Z.; Zhang, W.; Zhou, J.; Yang, C.; Luo, M.; Yang, Y.; Li, Y.; Gao, P.; Guo, S. Iridium-tungsten alloy nanodendrites as pH-universal water-splitting electrocatalysts. *ACS Cent. Sci.* **2018**, *4*, 1244−1252.

(18) Cheng, N.; Stambula, S.; Wang, D.; Banis, M. N.; Liu, J.; Riese, A.; Xiao, B.; Li, R.; Sham, T.-K.; Liu, L.-M.; Botton, G. A.; Sun, X. Platinum single-atom and cluster catalysis of the hydrogen evolution reaction. *Nat. Commun.* **2016**, DOI: 10.1038/ncomms13638.

(19) Panda, C.; Menezes, P. W.; Yao, S.; Schmidt, J.; Walter, C.; Hausmann, J. N.; Driess, M. Boosting electrocatalytic hydrogen evolution activity with a $NiPt_3$@NiS heteronanostructure evolved from a molecular nickel-platinum precursor. *J. Am. Chem. Soc.* **2019**, *141*, 13306−13310.

(20) Yu, W.; Porosoff, M. D.; Chen, J. G. Review of Pt-based bimetallic catalysis: from model surfaces to supported catalysts. *Chem. Rev.* **2012**, *112*, 5780−5817.

(21) Markovica, N. M.; Sarraf, S. T.; Gasteiger, H. A.; Ross, P. N. Hydrogen electrochemistry on platinum low-index single-crystal surfaces in alkaline solution. *J. Chem. Soc., Faraday Trans.* **1996**, *92*, 3719−3725.

(22) Mahmood, J.; Li, F.; Jung, S.-M.; Okyay, M. S.; Ahmad, I.; Kim, S.-J.; Park, N.; Jeong, H. Y.; Baek, J.-B. An efficient and pH-universal ruthenium-based catalyst for the hydrogen evolution reaction. *Nat. Nanotechnol.* **2017**, *12*, 441−446.

(23) Yao, Q.; Huang, B.; Zhang, N.; Sun, M.; Shao, Q.; Huang, X. Channel-rich RuCu nanosheets for pH-universal overall water splitting electrocatalysis. *Angew. Chem., Int. Ed.* **2019**, *58*, 13983−13983.

(24) Engstrom, J. R.; Tsai, W.; Weinberg, W. H. The chemisorption of hydrogen on the (111) and (110)-(1 × 2) surfaces of iridium and platinum. *J. Chem. Phys.* **1987**, *87*, 3104−3119.

(25) Li, F.; Han, G.-F.; Noh, H.-J.; Jeon, J.-P.; Ahmad, I.; Chen, S.; Yang, C.; Bu, Y.; Fu, Z.; Lu, Y.; Baek, J.-B. Balancing hydrogen adsorption/desorption by orbital modulation for efficient hydrogen

DOI: 10.1021/acsomega.9b03550
ACS Omega 2020, 5, 31−40

evolution catalysis. *Nat. Commun.* **2019**, DOI: 10.1038/s41467-019-12012-z.

(26) Chianelli, R. R.; Berhault, G.; Raybaud, P.; Kasztelan, S.; Hafner, J.; Toulhoat, H. Periodic trends in hydrodesulfurization: in support of the Sabatier principle. *Appl. Catal., A* **2002**, *227*, 83−96.

(27) Wu, X.; Feng, B.; Li, W.; Niu, Y.; Yu, Y.; Lu, S.; Zhong, C.; Liu, P.; Tian, Z.; Chen, L.; Hu, W.; Li, C. M. Metal-support interaction boosted electrocatalysis of ultrasmall iridium nanoparticles supported on nitrogen doped graphene for highly efficient water electrolysis in acidic and alkaline media. *Nano Energy* **2019**, *62*, 117−126.

DOI: 10.1021/acsomega.9b03550
ACS Omega 2020, 5, 31−40